NAVAL POSTGRADUATE SCHOOL

MONTEREY, CALIFORNIA

THESIS

OPTIMAL INTERDICTION OF AN ADAPTIVE SMUGGLER

by

Daniel L. Bessman

September 2010

Thesis Advisor:	Johannes O. Royset
Second Reader:	Javier Salmerón

Approved for public release; distribution is unlimited

THIS PAGE INTENTIONALLY LEFT BLANK

REPORT DOCUMENTATION PAGE			*Form Approved OMB No. 0704-0188*
Public reporting burden for this collection of information is estimated to average 1 hour per response, including the time for reviewing instruction, searching existing data sources, gathering and maintaining the data needed, and completing and reviewing the collection of information. Send comments regarding this burden estimate or any other aspect of this collection of information, including suggestions for reducing this burden, to Washington headquarters Services, Directorate for Information Operations and Reports, 1215 Jefferson Davis Highway, Suite 1204, Arlington, VA 22202-4302, and to the Office of Management and Budget, Paperwork Reduction Project (0704-0188) Washington DC 20503.			
1. AGENCY USE ONLY ***(Leave blank)***	**2. REPORT DATE** September 2010	**3. REPORT TYPE AND DATES COVERED** Master's Thesis	
4. TITLE AND SUBTITLE Optimal Interdiction of an Adaptive Smuggler		**5. FUNDING NUMBERS**	
6. AUTHOR(S) Daniel L. Bessman			
7. PERFORMING ORGANIZATION NAME(S) AND ADDRESS(ES) Naval Postgraduate School Monterey, CA 93943-5000		**8. PERFORMING ORGANIZATION REPORT NUMBER**	
9. SPONSORING /MONITORING AGENCY NAME(S) AND ADDRESS(ES) N/A		**10. SPONSORING/MONITORING AGENCY REPORT NUMBER**	
11. SUPPLEMENTARY NOTES The views expressed in this thesis are those of the author and do not reflect the official policy or position of the Department of Defense or the U.S. Government.			
12a. DISTRIBUTION / AVAILABILITY STATEMENT Approved for public release, distribution is unlimited.		**12b. DISTRIBUTION CODE**	

13. ABSTRACT (maximum 200 words)

Counterdrug operations are of national interest to the U.S. and our allies because the illegal production and trafficking of drugs threatens U.S. national security and undermines security and stability in Latin America. Since law enforcement tasked with counterdrug operations is not given enough platforms to search every location at all times, they must decide how to employ their scarce platforms. To assist law enforcement, we develop a defender-attacker optimization model that utilizes actionable intelligence to coordinate the simultaneous, cooperative disposition of law enforcement platforms in an optimal manner against a smuggler. The model utilizes stochastic dynamic programming to represent an intelligent smuggler, who has the ability to reevaluate his remaining path at decision points along his journey, based on knowledge obtained en route and expectations previously derived. The model employs Global Benders' Decomposition to determine the optimal placement of three different types of law enforcement platforms simultaneously prosecuting one of three possible types of smuggler. We show that such computations cannot be performed fast enough to be used in a tactical decision aid, since they typically require in excess of two hours. Upon further analysis using our model, we determine a large number of defender missions do not have a substantial impact on the attacker's risk. Based on the results of our model, we believe further algorithmic development is needed for implementation into a tactical decision aid to assist in counter drug operations.

14. SUBJECT TERMS Stochastic Optimization, Dynamic Programming, Defender-Attacker Optimization, Global Bender's Decomposition, Search and Detection			**15. NUMBER OF PAGES** 57
			16. PRICE CODE
17. SECURITY CLASSIFICATION OF REPORT Unclassified	**18. SECURITY CLASSIFICATION OF THIS PAGE** Unclassified	**19. SECURITY CLASSIFICATION OF ABSTRACT** Unclassified	**20. LIMITATION OF ABSTRACT** UU

NSN 7540-01-280-5500 Standard Form 298 (Rev. 2-89)
Prescribed by ANSI Std. 239-18

THIS PAGE INTENTIONALLY LEFT BLANK

Approved for public release; distribution is unlimited

OPTIMAL INTERDICTION OF AN ADAPTIVE SMUGGLER

Daniel L. Bessman
Lieutenant Commander, United States Navy
B.S., United States Naval Academy, 1999

Submitted in partial fulfillment of the
requirements for the degree of

MASTER OF SCIENCE IN OPERATIONS RESEARCH

from the

NAVAL POSTGRADUATE SCHOOL
September 2010

Author: Daniel L. Bessman

Approved by: Dr. Johannes O. Royset
Thesis Advisor

Dr. Javier Salmerón
Second Reader

Dr. Robert F. Dell
Chairman, Department of Operations

THIS PAGE INTENTIONALLY LEFT BLANK

ABSTRACT

Counterdrug operations are of national interest to the U.S. and our allies because the illegal production and trafficking of drugs threatens U.S. national security and undermines security and stability in Latin America. Since law enforcement tasked with counterdrug operations is not given enough platforms to search every location at all times, they must decide how to employ their scarce platforms. To assist law enforcement, we develop a defender-attacker optimization model that utilizes actionable intelligence to coordinate the simultaneous, cooperative disposition of law enforcement platforms in an optimal manner against a smuggler. The model utilizes stochastic dynamic programming to represent an intelligent smuggler, who has the ability to reevaluate his remaining path at decision points along his journey, based on knowledge obtained en route and expectations previously derived. The model employs Global Benders' Decomposition to determine the optimal placement of three different types of law enforcement platforms simultaneously prosecuting one of three possible types of smuggler. We show that such computations cannot be performed fast enough to be used in a tactical decision aid, since they typically require in excess of two hours. Upon further analysis using our model, we determine a large number of defender missions do not have a substantial impact on the attacker's risk. Based on the results of our model, we believe further algorithmic development is needed for implementation into a tactical decision aid to assist in counter drug operations.

THIS PAGE INTENTIONALLY LEFT BLANK

TABLE OF CONTENTS

THIS PAGE INTENTIONALLY LEFT BLANK

LIST OF FIGURES

THIS PAGE INTENTIONALLY LEFT BLANK

LIST OF TABLES

THIS PAGE INTENTIONALLY LEFT BLANK

LIST OF ACRONYMS AND ABBREVIATIONS

AM	Attacker's Model
AP	Attacker's Problem
C-130	Airborne early warning aircraft *Hercules*
CD	Counterdrug operations
DAM	Defender-Attacker Model
FFG	*Oliver Hazard Perry*-class frigate
FOL	Forward Operating Location
GAMS	General Algebraic Modeling System
GLBD	Global Benders Decomposition
JIATF-S	Joint Interagency Task Force South
MP-GLBD	Global Benders Decomposition Master Problem
ODP	Optimal Detection Problem
P-3	Maritime patrol aircraft *Orion*
SPSS	Self Propelled Semi-Submersible
SOUTHCOM	United States Southern Command
TD-OSP	Temporal Dependence One-Step Spatial Dependence Algorithm

THIS PAGE INTENTIONALLY LEFT BLANK

EXECUTIVE SUMMARY

Maritime drug smugglers in the Eastern Pacific Ocean have historically used a combination of seacraft to smuggle contraband. These seacraft include Go-Fast power boats, Panga commercial fishing vessels, and Self Propelled Semi-Submersibles. To defend against smuggling, law enforcement participating in counterdrug operations employ platforms such as *Oliver Hazard Perry*-class frigates and the maritime patrol aircraft *Orion* and *Hercules*. But law enforcement faces the predicament of having only a few available platforms at any given time, and searching for a single smuggler can tie up many law enforcement platforms. Current law enforcement strategy relies heavily on actionable intelligence, with consideration of geography and weather to help determine the most advantageous positioning of their platforms. There is no computer-based tactical tool to aid these platform employment decisions.

We introduce a tactical decision aid to recommend placement of the limited law enforcement platforms. This planning aid will provide optimal placement through mission assignment while considering the intelligent response of the smugglers. A successful operation against a smuggler requires detection, monitoring, tracking, and interdiction. This thesis addresses detection only.

We develop a defender-attacker optimization model to optimally place law enforcement platforms in order to maximize the smuggler's minimum expected risk, from the time and location the smuggler is spotted. We assume the smuggler to be intelligent and have imperfect knowledge of law enforcement platform placement, but that he is aware that there is law enforcement that must be avoided. Additionally, the smuggler only gains perfect knowledge of scenarios and defender placement on immediate path segments, just before he decides to take that path. We demonstrate our defender-attacker model prescribes the optimal law enforcement missions to maximize the smuggler's risk, but is not fast enough to be used in a tactical decision aid.

THIS PAGE INTENTIONALLY LEFT BLANK

ACKNOWLEDGEMENTS

I am deeply indebted to my advisor, Dr. Johannes Royset. This thesis would not have been possible without your guidance and patience. Allowing me to take on water, but not enough to drown, made this journey an incredible learning experience. It was my honor to work with you.

This thesis would not have been possible without the light in my life, Lorene. Thank you for standing by me on this journey and enduring many children's birthday parties, play dates, and other social events while I battled the computer. I am truly blessed.

THIS PAGE INTENTIONALLY LEFT BLANK

I. INTRODUCTION

A. OVERVIEW

Counterdrug operations (CD) are of great interest and high operational importance to the United States. Successful CD involve four phases: detection, monitoring, tracking, and interdiction, and are the operational background to this thesis, which addresses detection only. We develop a defender-attacker optimization model utilizing actionable intelligence to coordinate the simultaneous, cooperative disposition of limited law enforcement platforms in against an intelligent smuggler. We define an intelligent smuggler as someone who has the ability to reevaluate his remaining path at decision points along his journey, based on knowledge obtained en route and expectations previously derived. The model developed in this thesis encompasses three different types of law enforcement platforms and three different types of smuggler seacraft. We implement the model for several cases that take place in the Eastern Pacific Ocean. With further algorithmic development, the model could be implemented in a tactical decision aid and produce real-time recommendations for courses of actions to law enforcement.

B. THE DRUG SMUGGLING THREAT

Ninety percent of the cocaine and forty-seven percent of the heroin that reaches the United States originates in or passes through Colombia. Illegal drugs kill more than 21,000 Americans every year and result in the loss of "more than $160 billion in revenue" (United States Southern Command, 2010). U.S. Southern Command (SOUTHCOM) has been designated as the lead U.S. government agency to counter drug smuggling. The principal interdiction arm of SOUTHCOM is Joint Interagency Task Force South (JIATF-S), which is composed of representatives from several U.S., European, and Latin American law enforcement agencies. By collaborating with other agencies and nations to detect, monitor, track, and interdict drug runners, coordinated efforts have disrupted the flow of more than 215 metric tons of cocaine in 2009, with similar numbers recorded in 2007 and 2008 (SOUTHCOM, 2010).

Drug smugglers continue to adapt to law enforcement successes. Not only have their strategies and tactics changed, but so have their seacraft. These include the Self-Propelled Semi-Submersible (SPSS) (Figure 1), the Panga fishing boat (Figure 2), and the Go-Fast powerboat (Figure 3).

Figure 1. Self Propelled Semi-Submersible (SPSS) (From Wikipedia.org 2010).

Figure 2. Panga Fishing Boat (From Travelismo.com 2010).

Figure 3. Go-Fast Powerboat (From Wikipedia.org 2010).

The SPSS represents the emerging sophistication and innovation of drug traffickers to adapt to U.S. and regional counter-drug capabilities. The hull of an SPSS rises only about a foot above the waterline, so the craft is hard to see from a distance, leaves little wake, and produces only a small radar signature. SOUTHCOM, the U.S. Coast Guard, and regional officials consider the SPSS a serious threat to U.S. and regional security. Navy Admiral Jim Stavridis, former Commander, SOUTHCOM, stated, "What worries me [about the SPSS] is if you move that much cocaine, what else can you put in that semi-submersible. Can you put a weapon of mass destruction in it?" (SOUTHCOM, 2010). With limited number of law enforcement platforms, and a large area of water to defend, one way to help find drug smuggling seacraft is with smarter methods of employing the enforcement platforms.

Currently, there is no tactical computer-based tool to aid mission planners performing counterdrug operations (private communication with Sellers, 2010). This thesis develops and implements an attacker-defender model for optimally employing search platforms such as *Oliver Hazard Perry*-class frigates (FFGs) (Figure 4) and the maritime patrol aircraft *Orion* (P-3s) (Figure 5) and *Hercules* (C-130s) (Figure 6) in maritime counterdrug operations.

Figure 4. U.S. Navy *Oliver Hazard Perry*-class Frigate (From defenseindustrydaily.com 2010).

Figure 5. U.S. Department of Homeland Security P-3 *Orion* Airborne Early Warning Aircraft (From Wikipedia.org 2010).

Figure 6. U.S. Coast Guard C-130 *Hercules* Maritime Patrol Aircraft (From Wikimedia.org 2010).

C. RELATED WORK

Defender-attacker models have been used to model counter-smuggling efforts. Wood (1993) constructs a defender-attacker model to best apportion a limited number of SOUTHCOM resources to reduce the flow of drugs through South America. Dimitrov et al. (2008) implement a stochastic defender-attacker model to provide optimal radiation detector locations to counter nuclear smuggling. Pfeiff (2009) uses a defender-attacker model to recommend the optimal placement and disposition of JIATF-S platforms. Washburn and Wood (1995) view the problem of placing defender(s) as a simultaneous play, two-person zero-sum game and develop corresponding algorithms based on network models. In the above papers, the attacker (the smuggler) is trying to minimize his risk while the defender (law enforcement) is trying to maximize that same risk (i.e., a max-min problem). However, none of these papers model the attacker as intelligent in the sense defined above, yet it may be more realistic to view him as such.

In this thesis, we develop models that deal with an intelligent attacker. To the author's knowledge, there is only one attempt along this line in the literature. Dimitrov and Morton (2008) formulate a stochastic defender-attacker model using dynamic programming where law enforcement's goal is to deploy stationary detectors to minimize the probability that a smuggler avoids detection. The smuggler is not fully in control of his movement and obeys a Markov decision process. Specifically, the smuggler solves a stochastic shortest-path problem where at each node in a network, the smuggler selects a probability distribution that determines the smuggler's next node. In this thesis, we adopt a similar model but consider movable sensors and a different stochastic shortest-path problem where the smuggler is in full control of his movement, but has incomplete information about the risks along various routes as described in detail below.

D. THESIS ORGANIZATION

The remainder of this thesis is organized in the following manner: Chapter II presents the formulation of a defender-attacker model, and the algorithms we use to solve it. Chapter III discusses numerical results. Chapter IV summarizes this research and presents the conclusions. The appendices provide assumptions and rationale we use to determine the attacker's risk. Specifically, Appendix A provides details of the derivation of the probabilities of detection for each of law enforcement's platforms against each of the smuggler's seacraft. Appendix B provides details of the atmospheric conditions and their affect on the probabilities of detection mentioned above.

II. MODEL DEVELOPMENT

A. OVERVIEW

In this chapter, we present a defender-attacker optimization model which coordinates the simultaneous, cooperative disposition of law enforcement platforms in an optimal manner against an intelligent smuggler. We begin by discussing a network describing the movement possibilities of the smuggler. Then we formulate the smuggler's problem as a stochastic shortest-path problem and formulate a problem that optimally allocates law enforcement platforms. We conclude this chapter with a brief discussion of our employment of Global Benders' Decomposition Algorithm for solving the resulting model.

B. SETTING AND PROBLEM STATEMENT

We consider a situation in which a smuggler seeks to move from a node *s* to a node *d* in a directed graph in such a way that his expected risk, as defined precisely below, is minimized and his travel time does not exceed a given threshold. Each node in the graph represents a physical location and each arc represents the possibility of movement between two nodes for the smuggler; see Figure 7, which depicts a simple network in the eastern Pacific Ocean. We refer to the smuggler as the *attacker*.

Each arc is associated with a set of scenarios, each of which occurs with a known probability. The scenario represents a set of conditions that the attacker may face. Each scenario is associated with a probability of detection, which as explained below, is referred to as "risk" after a logarithmic transformation. The set of scenarios on an arc defines all possible conditions the attacker may face on the arc. We assume that the occurrence of scenarios on any two arcs is independent, i.e., the knowledge about the occurrence of a scenario on one arc does not provide any information about the probability of a specific scenario occurring on another arc.

The attacker does not know which scenario is taking place on an arc until he arrives at the tail node of the arc. At that point, he learns the scenario on the arc and therefore his probability of avoiding detection if he traverses that arc. An arc is also associated with a travel time that may depend on the scenario. These scenarios occur according to a probability distribution. The attacker would like to travel from *s* to *d* with minimum expected risk, subject to a total time constraint. He does not need to commit to a path *a priori*. Rather, he adapts a policy where at each node he only selects the next arc to traverse. The attacker would like to determine a policy for this arc selection that minimizes his expected risk, while satisfying the time constraint. We call this the Attacker's Problem (AP).

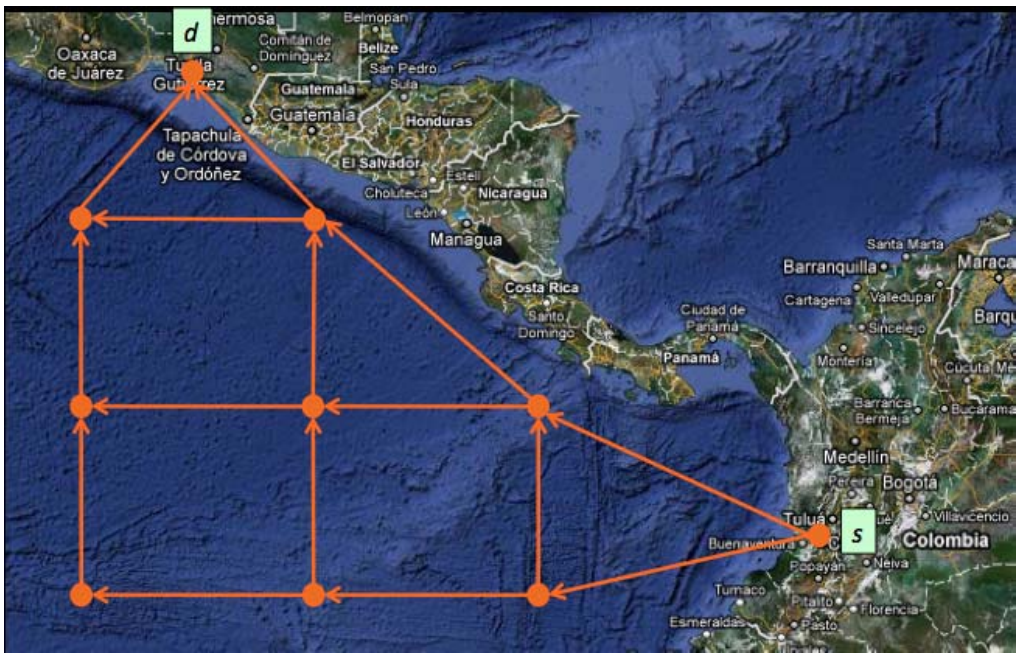

Figure 7. Eastern Pacific Ocean with a graph defining possible paths for a smuggler, (From Google Maps, 2010).

The defender has a number of search platforms, each of which he assigns to a *mission*. A mission is a set of arcs that a search platform may search in an attempt to detect the attacker. Due to operational constraints, the defender must assign all search platforms to missions prior to the departure of the smuggler from node *s*. Hence, the defender is unable to capitalize on information acquired during the search operation. The presence or absence of a search platform on an arc may influence both the risk in the

scenarios and the probability of the scenarios for the attacker on that arc. The defender's goal is to maximize the attacker's minimum expected risk. We call this problem the Optimal Detection Problem (ODP). We formulate the ODP as a defender-attacker model, develop an algorithm for its solution, and incorporate the algorithm in a prototype of a decision aid.

C. MODEL FORMULATION

1. The Attacker

We formulate ODP by first considering AP for a given set of missions for the defender. The next section gives the full model.

The attacker would like to travel from *s* to *d* within a certain time window and without being detected by the defender. However, both travel times and detection probabilities are uncertain, and represented by "scenarios." Since the attacker plans to repeat similar travel many times, for planning purposes, he aims to minimize the *expected* probability of detection. The attacker's movements are modeled using a *physical graph* $G=(N,A)$, with an explicit representation of time added. The physical graph comprises physical locations, represented by nodes, $i, j \in N$, which are connected by arcs, $(i,j) \in A$, defining potential movements between nodes. The set A may include self-loops of the form $(i,i) \in A$. Time is discretized into time periods t = 0, 1, 2, …. The attacker must depart node *s* during time periods t = 0, 1, …., $t_{0,\max}$ and must arrive at node *d* no later than $t_{\max}$ time periods after he departs node *s*.

Each arc $(i, j) \in A$ and time period t is associated with a set of *scenarios* Ω_{ijt}. A scenario is a possible condition the attacker may experience while transiting an arc at a particular time period. As we see below, the attacker's travel time and his probability of avoiding detection on the arc may depend on the scenario he realizes. The scenario $\omega_{ijt} \in \Omega_{ijt}$ occurs with probability $q_{ijt\omega_{ijt}}$, hence $\sum_{\omega_{ijt} \in \Omega_{ijt}} q_{ijt\omega_{ijt}} = 1$. The attacker has a probability $p_{ijt\omega_{ijt}}$ of surviving (i.e., avoiding detection) while traveling along arc

$(i, j) \in A$ if he departs node *i* at time t and scenario $\omega_{ijt} \in \Omega_{ijt}$ is realized. That travel takes $\tau_{ijt\omega_{ijt}}$ time periods, with $\tau_{ijt\omega_{ijt}}$ being a positive integer. We assume that the detection events are independent. Let $r_{ijt\omega_{ijt}} \equiv -\log p_{ijt\omega_{ijt}}$ denote the corresponding *risk*.

The goal of the attacker is to minimize the expected risk associated with traveling from node *s* to node *d* given the following ability to observe scenarios. In general, the attacker is unaware of the scenario he will face at a particular arc and time. However, if the attacker is located at node *i* in time period *t*, then he will observe a specific scenario $\omega_{ijt} \in \Omega_{ijt}$ for all $j \in F_i$, where $F_i = \{ j \in N \mid (i, j) \in A \}$ is the forward star of node *i*. This observation is made prior to making a decision about which node to proceed to from *i*.

The Attacker Model (AM) takes the following form:

Indices and Index Sets

$i, j \in N$	nodes in physical graph
$(i, j) \in A$	arcs in physical graph
F_i	arcs in the forward star of node $i \in N$ in the physical graph
t	time period, $t =$ 0, 1, ….,
$\omega_{ijt} \in \Omega_{ijt}$	scenario on arc $(i, j) \in A$ in time period t, $\omega_{ijt} \in \Omega_{ijt}$
$\bar{\omega}_{it} \in \bar{\Omega}_{it}$	scenario vector at node i in time period t, $\bar{\omega}_{it} = (\omega_{ijt})_{j \in F_i}$
t_0	time period of departure from node *s*, with $t_0 = -1$ indicating not yet departed, $t_0 = -1, 0, 1, \ldots, t_{0,\max}$

Data

s	start node in physical graph
d	destination node in physical graph
$q_{ijt\omega_{ijt}}$	probability of scenario $\omega_{ijt} \in \Omega_{ijt}$ on arc $(i, j) \in A$ in time period t; $\sum_{\omega_{ijt} \in \Omega_{ijt}} q_{ijt\omega_{ijt}} = 1$

$\bar{q}_{it}(\bar{\omega}_{it})$ probability of scenario vector $\bar{\omega}_{it}$ at node i in time period t; $\bar{q}_{it}(\bar{\omega}_{it}) = \prod_{j \in F_i} q_{ijt\omega_{ijt}}$

$p_{ijt\omega_{ijt}}$ probability that the attacker survives arc $(i, j) \in A$ if the attacker starts traversing this arc in time period t in scenario $\omega_{ijt} \in \Omega_{ijt}$

$r_{ijt\omega_{ijt}}$ risk to the attacker on arc $(i, j) \in A$ if starting traversing the arc in time period t in scenario $\omega_{ijt} \in \Omega_{ijt}$; $r_{ijt\omega_{ijt}} = -\log p_{ijt\omega_{ijt}}$

$\tau_{ijt\omega_{ijt}}$ travel time from $i \in N$ to $j \in N$ if the attacker starts traversing arc $(i, j) \in A$ in time period t in scenario $\omega_{ijt} \in \Omega_{ijt}$

$t_{\max}$ maximum allowable travel time from *s* to *d*

$t_{0,\max}$ maximum allowable waiting time at *s*

Function

$V(i,t,t_0)$ Minimum expected risk to travel from node i to node d starting in time period t and given that the attacker departed node *s* at time period t_0. This function is defined as follows:

(Bellman Equations for the attacker's decisions)

I. If $t_0 = -1, i = s,$ and $t \le t_{0,\max}$ (attacker has not started):

$$V(s,t,-1) = \sum_{\bar{\omega}_{st} \in \bar{\Omega}_{st}} \bar{q}_{st}(\bar{\omega}_{st}) \left[\min \left\{ r_{sst\omega_{sst}} + V(s,t+1,-1), \min_{j \in F_s - \{s\}} r_{sjt\omega_{sjt}} + V\left(j, t + \tau_{sjt\omega_{sjt}}, t\right) \right\} \right].$$

II. If $t_0 \ge 0, i \ne d,$ and $t - t_0 \le t_{\max}$ (attacker has not reached destination):

$$V(i,t,t_0) = \sum_{\bar{\omega}_{it} \in \bar{\Omega}_{it}} \bar{q}_{it}(\bar{\omega}_{it}) \left[\min_{j \in F_i} r_{ijt\omega_{ijt}} + V\left(j, t + \tau_{sjt\omega_{sjt}}, t_0\right) \right].$$

(Absorbing States)

III. If $t_0 = -1, i = s,$ and $t > t_{0,\max}$ (attacker has exceeded start time):

$V(s,t,-1) = \infty.$

IV. If $t_0 \geq 0$ and $t - t_0 > t_{\max}$ (attacker has exceeded finish time):
$V(i, t, t_0) = \infty.$

V. If $t_0 \geq 0, i = d,$ and $t - t_0 \leq t_{\max}$ (attacker has reached destination):
$V(d, t, t_0) = 0.$

Formulation

$$\text{AM:} \quad \text{Determine } V(s, 0, -1) \tag{1}$$

AM includes five versions of Bellman's equation. Version I deals with the situation when the attacker has not departed the start node *s*. Version II represents the situation where the attacker has not reached its destination. Versions III and IV assign an infinite value when the attacker has not departed its start node within the allowable time window or when it does not reach the destination within time. Version V assigns zero to a state corresponding to the attacker's arrival at the destination within the time window.

2. The Defender-Attacker Model

The defender influences the attacker's risk by changing the probabilities $q_{ijt\omega_{ijt}}$ and risks $r_{ijt\omega_{ijt}}$ associated with scenarios on arcs. Specifically, the defender assigns each search platform a mission. The mission specifies a sequence of arcs, one for each time period, which the search platform will examine. Typically, if a search platform examines an arc, then the risk is high for the attacker on that arc. Therefore, the presence or absence of the defender determines risk. Scenarios on the arcs, such as environmental conditions, also determine risk. This section formulates an optimization model that maximizes the minimum expected risk to the attacker by assigning a mission to each platform. We refer to this model as the Defender-Attacker Model (DAM).

Indices and Index Sets

$l \in L$ defender platform

$m \in M_l$ mission that platform *l* may execute

Decision Variables

x_{lm} 1 if platform *l* executes mission $m \in M_l$; 0 otherwise

$x = (x_{lm})_{l \in L, m \in M_l}$ is the mission plan

Functions

$q_{ijt\omega_{ijt}}(x)$ probability of scenario $\omega_{ijt} \in \Omega_{ijt}$ on arc $(i, j) \in A$ in time period *t* given mission plan x; $\sum_{\omega_{ijt} \in \Omega_{ijt}} q_{ijt\omega_{ijt}}(x) = 1$

$r_{ijt\omega_{ijt}}(x)$ risk of scenario $\omega_{ijt} \in \Omega_{ijt}$ on arc $(i, j) \in A$ in time period *t* given mission plan x

$f(x)$ minimum expected risk, given mission plan x, to travel from node *s* to node *d* departing *s* no later than time period $t_{0,\max}$ and arriving at *d* no later than $t_{\max}$ time periods after departing *s*; $f(x) = V^x(s, 0, -1)$, where $V^x(s, 0, -1)$ is defined identical to $V(s, 0, -1)$, see Equation (1), except with $q_{ijt\omega_{ijt}}$ replaced by $q_{ijt\omega_{ijt}}(x)$ and $r_{ijt\omega_{ijt}}$ replaced by $r_{ijt\omega_{ijt}}(x)$.

Formulation

$$\text{DAM:} \quad \max_x f(x) \tag{2}$$

$$\text{s.t.} \sum_{m \in M_l} x_{lm} \leq 1 \quad \forall l \tag{3}$$

$$x_{lm} \in \{0,1\} \quad \forall l, m \tag{4}$$

The DAM objective function (2) maximizes the attacker's minimum expected risk of travel from node *s* to node *d*, given that the attacker departs *s* no later than time period $t_{0,\max}$ and arrives at *d* no later than $t_{\max}$ time periods after departing *s*. Constraints (3) and (4) require that each defensive platform carry out at most one mission.

3. Algorithm

A standard max-min formulation can be solved using Benders Decomposition, which builds a concave piecewise linear function of the function being maximized (Benders, 1962). But, to use Benders Decomposition, the function must be concave, which may not be the case for DAM. Therefore, we use Global Benders Decomposition (GLBD) (Salmerón et al., 2009). The AM is the GLBD subproblem and could be solved by dynamic programming. However, we plan to utilize the more efficient all-to-one label-correcting Temporal Dependence One-Step Spatial Dependence (TD-OSP) Algorithm developed by Waller and Ziliaskopoulos (2002). This algorithm finds a solution with the least expected risk in pseudo-polynomial time on acyclic graphs. The GLBD master problem is a linearization of DAM given in the *K*-th iteration by

$$\text{MP-GLBD:} \quad \max z \tag{5}$$

$$\text{s.t. } f(\hat{x}^k) + \sum_{l \in L} \sum_{m \in M_l} \alpha_{lm}^k \left(x_{lm} - \hat{x}_{lm}^k \right) \geq z \quad \forall k = 1, 2, 3, \ldots K \tag{6}$$

$$\sum_{m \in M_l} x_{lm} \leq 1 \quad \forall l \tag{7}$$

$$x_{lm} \in \{0,1\} \quad \forall l, m \tag{8}$$

where $\hat{x}_{lm}^k$ is the solution examined in the *k*-th AM subproblem and $f(\hat{x}^k)$ is the corresponding optimal value of the AM subproblem. Constraint (6) is a set of linear approximations of the objective function in DAM. Specifically, α_{lm}^k, $l \in L$, $m \in M_l$, are coefficients such that $f(\hat{x}^k) + \sum_{l \in L} \sum_{m \in M_l} \alpha_{lm}^k \left(x_{lm} - \hat{x}_{lm}^k \right) \geq f(x)$ for all $x = \left(x_{lm} \right)_{l \in L, m \in M_l}$ such that (7) and (8) hold. In the next chapter, we consider a specific situation where such an upper bound can easily be computed. GLBD consists of alternating between solving the AM subproblem and MP-GLBD master problem. The subproblem provides a lower bound on the optimal value of DAM and MP-GLBD an upper bound.

III. RESULTS AND ANALYSIS

A. OVERVIEW

This chapter is organized in the following way: Section B presents an overview and the development of six operational cases JIATF-S operators could face any day. In Section C, we analyze the six cases, and discuss the results and insights of this analysis. Section D uses two of the six cases to determine the number of missions in which the defender can increase the attacker's risk more than ten percent.

We implement DAM using Visual Basic for Applications (VBA) to solve AM and General Algebraic Modeling System (GAMS) with the CPLEX solver to solve MP-GLBD. The implementation was run on a Dell Precision desktop computer T7400 with an Intel Xenon 3.16GHz CPU with 3.25GB RAM, with the Windows XP Professional operating system.

B. OPERATIONAL CASES

The numerical case study presented in this chapter includes a baseline situation, and several case variations of this baseline situation for sensitivity analysis and evaluation of the robustness of the baseline situation's results and insights.

1. Baseline Situation

The baseline situation takes place in the Eastern Pacific Ocean, bounded between latitude lines 17° North latitude and 7° South latitude and 77° and 104° West longitude, encompassing 1680 nm "wide" by 1500 nm "high." We discretize this area into 700 60nm by 60nm square cells, though only a small portion of cells are used in any given situation; see Figure 8. Each cell represents a node in the physical graph in DAM. The origin of this map occurs at the lower left-hand corner, with the numbers on the bottom referring to x-coordinates and the numbers on the left referring to y-coordinates of attacker seacraft and defender platforms. We display the coast of Colombia on the lower right and the coast of Mexico on the upper left. Cell "A" in Figure 8 is the attacker, cell

"C" is the Comalapa, Ecuador Forward Operating Location (FOL) and the only cell where the defender's P-3 and C-130 platforms originate, and cell "F" is the defender's FFG. The FFG's position is dynamic and can occur in any of the white cells. All black cells, and cell "C", represent land in Figure 8. The grid allows for many possible "Contact Reports," but in any one case, only a portion of the map is actually used and generated by the models.

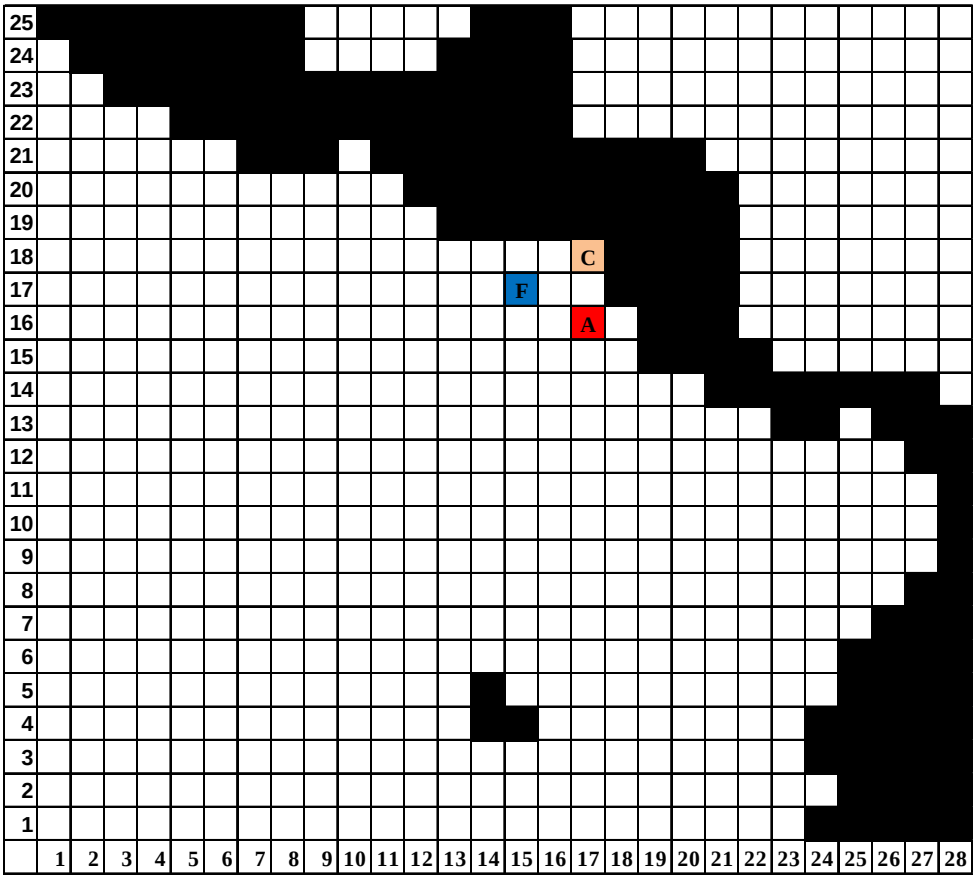

Figure 8. Snapshot of Eastern Pacific Ocean in Microsoft Excel. Each cell is a 60 nautical mile square. We display the coast of Colombia on the lower right and the coast of Mexico on the upper left. Cell "A" is the attacker, cell "C" is the Comalapa, Ecuador FOL (the only cell where the defender's P-3 and C-130 platforms originate), and cell "F" is the defender's FFG. All black cells, and cell "C", represent land.

The attacker's start node in the physical graph, s, is coordinate pair (17, 16) and determined by translating his latitude-longitude position into a cell in Figure 8. There is no delay, $t_{0,\max} = 0$, in reporting the attacker at s and the JIATF-S operator receiving this

information. We assume that JIATF-S has intelligence that the attacker aims for land coordinate (7, 21) and set *d* to be the node in the physical graph that corresponds to that coordinate. In general, uncertainty about the attacker's destination can be reflected by adding additional arcs in the physical graph and letting *d* be a "super sink."

We assume the attacker desires forward movement at all times. Therefore, we model the attacker with the possible movement to three immediate neighboring cells (left, right, and forward) in a single time period or waiting in the current cell for one time period. Each such move or waiting is represented by an arc in the physical graph. We do not model backward or diagonal movement. This results in the physical graph having a maximum forward star of size four. The forward star is not always size four due to land constraints. There are two possible scenarios that can occur on each arc and time period, i.e., $\Omega_{ijt} \in \{1,2\} \ \forall ijt$. Let S_{lm} be the set of triplets (i,j,t) such that platform *l* on mission *m* searches arc (i,j) during time period *t*. When no defensive platform is present on (i,j) during time period *t*, the probability of scenario 1 occurring equals 0.7, i.e., $q_{ijt1}(x)$=0.7 when x_{lm}=0 for all *l* and *m* such that $(i,j,t) \in S_{lm}$. The probability of scenario 2 occurring equals 0.3, i.e., $q_{ijt2}(x)$=0.3 when x_{lm}=0 for all *l* and *m* such that $(i,j,t) \in S_{lm}$. When at least one defender platform is present on arc (i,j) during time period *t*, then the probabilities of scenarios 1 and 2 occurring equal 0.9 and 0.1, respectively, i.e., $q_{ijt1}(x)$=0.9 and $q_{ijt2}(x)$=0.1 when x_{lm}=1 for at least one pair (l,m) such that $(i,j,t) \in S_{lm}$. We compute the risks, $r_{ijt1}(x)$ and $r_{ijt2}(x)$ using the information provided in Appendices A and B. Each type of attacker seacraft can traverse a square cell in one time period. Hence, $\tau_{ijt\omega_{ijt}}$=1 for all attacker seacraft, and a time period represents different amounts of time depending on the attacker's speed. We assume a constant speed of 6 knots for an SPSS, 15 knots for a Panga, and 25 knots for a Go-Fast.

The defender's initial FFG position is coordinate pair (15, 17) and both the P-3 and C-130 are located at coordinate pair (15, 17), the Comalapa FOL. These coordinates are determined by translating their latitude-longitude positions into a cell in Figure 8. We

determine the set of possible missions, M_l, that platform *l* may execute via time-distance calculations. These calculations begin by determining if the defender's platform can reach the tail of an arc before the attacker can reach that tail. If so, that arc will become a one-time period mission. Additionally, for every arc emanating from the forward star of a one-time period mission, the defender will add this arc to the original arc to become a two-time period mission. Missions continue to be made by adding arcs in the forward star for $t_{\max}$ time periods. We assume a constant speed of 15 knots for an FFG and 180 knots for both the P-3 and C-130.

We compute the cut coefficients α_{lm}^k in (6) by setting α_{lm}^k=0 if $\hat{x}_{lm}^k$=1 and otherwise set $\alpha_{lm}^k = \sum_{(i,j,t)\in S_{lm}} \left[q_{ijt1}(e_{lm}) r_{ijt1}(e_{lm}) + q_{ijt2}(e_{lm}) r_{ijt2}(e_{lm}) - q_{ijt1}(0) r_{ijt1}(0) - q_{ijt2}(0) r_{ijt2}(0) \right]$, where e_{lm} is the unit vector with components all zero except the (*l*,*m*)-component, which is unity. Effectively, α_{lm}^k equals the expected risk to an attacker that traverses arcs covered by platform *l* on mission *m*, minus the expected risk absent any defender. Under the assumption that a platform does not influence the probabilities of scenarios and risks on other arcs and time periods than those covered by the platform, it appears that this leads to a valid cut in (6). However, this thesis does not provide a formal proof.

2. Case Studies

The six case studies are defined as follows. In Case 1, the defender consists of one frigate (FFG) and we set time horizon $t_{\max}$ = 5 and $t_{0,\max}$ = 0, hence the attacker must depart immediately. In Case 2, the defender consists of one air platform (P-3) and we set $t_{\max}$ = 5 and $t_{0,\max}$ = 0. In Case 3, the defender consists of one frigate (FFG) and both air platforms (P-3 & C-130) and we set $t_{\max}$ = 5 and $t_{0,\max}$ = 0. In Case 4, the defender consists of one frigate (FFG) and we set $t_{\max}$ = 7 and $t_{0,\max}$ = 0. In Case 5, the defender consists of one air platform (P-3) and we set $t_{\max}$ = 7 and $t_{0,\max}$ = 0. In Case 6, the defender consists of one frigate (FFG) and both air platforms (P-3 & C-130) and we set $t_{\max}$ = 7 and $t_{0,\max}$ = 0. Table 1 summarizes the six cases and also gives the total number

of missions for all platforms, i.e., $\prod_l |M_l|$, where $|M_l|$ is the cardinality of M_l, and the minimum expected risk to the attacker in the absence of any defender for three attacker seacraft. We refer to this risk as the "inherent risk."

	Defender Platform(s)	$t_{\max}$	Total Number of Missions	SPSS Inherent Risk	Panga Inherent Risk	Go-Fast Inherent Risk
Case 1	FFG	5	266	2.551	3.470	4.232
Case 2	Air Platforms	5	284	2.551	3.470	4.232
Case 3	FFG & Air Platforms	5	21,454,496	2.551	3.470	4.232
Case 4	FFG	7	3,998	3.042	4.374	5.361
Case 5	Air Platforms	7	12,730	3.042	4.374	5.361
Case 6	FFG & Air Platforms	7	647 billion	3.042	4.374	5.361

Table 1. SPSS data for Cases 1-6. Column one shows the defender platforms available. Column two shows the number of time periods available to prosecute the attacker. Column three shows the total number of missions. Columns four, five, and six show the inherent risk for the SPSS, Panga, and Go-Fast, respectively.

C. RESULTS AND INSIGHTS

We solve DAM for the six cases described above, for each attacker seacraft, using GLBD with results summarized in Tables 2, 3, and 4. Column one shows the DAM solution time. Column two shows the total enumeration solution time (N/C = Not Computed), i.e., the time required to solve AM for all missions. Column three shows maximum risk obtained by GLBD within two hours of computation time. Column four shows the percentage increase in this risk over the inherent risk. Column five shows the optimal risk in DAM, computed by total enumeration when available. Column six shows the relative gap between maximum risk from GLBD after two hours and the optimal risk. Column seven shows the relative gap in GLBD after two hours of computing time.

	GLBD Solution Time (secs)	Total Enum. Time (secs)	GLBD Lower Bound	GLBD Increase Above Inherent	Optimal Risk	Gap between GLBD and Optimal	GLBD Gap
Case 1	502	51	2.595	1.7%	2.595	0%	0%
Case 2	522	280	2.964	16.2%	2.964	0%	0%
Case 3	> 7200	N/C	3.099	5.3%	N/C	N/C	1694%
Case 4	> 7200	4250	3.113	2.3%	3.182	2.2%	563%
Case 5	> 7200	13023	3.548	16.6%	3.760	5.6%	829%
Case 6	> 7200	N/C	3.542	16.4%	N/C	N/C	1399%

Table 2. Results of Cases 1-6 with SPSS. Column one shows the GLBD solution time. Column two shows the total enumeration solution time. Column three shows the GLBD Lower Bound. Column four shows the percentage that the GLBD risk raises the inherent risk. Column five shows the optimal risk computed by total enumeration. Column six shows the relative gap between the GLBD risk and the optimal risk. Column seven shows the relative GLBD gap.

	GLBD Solution Time (secs)	Total Enum. Time (secs)	GLBD Lower Bound	GLBD Increase Above Inherent	Optimal Risk	Gap between GLBD and Optimal	GLBD Gap
Case 1	503	53	3.862	11.3%	3.862	0%	0%
Case 2	522	303	3.970	14.4%	3.970	0%	0%
Case 3	> 7200	N/C	4.011	7.3%	N/C	N/C	999%
Case 4	> 7200	4160	4.411	0.9%	4.450	0.9%	422%
Case 5	> 7200	13016	4.782	11.6%	5.085	6.0%	617%
Case 6	> 7200	N/C	4.491	2.7%	N/C	N/C	1275%

Table 3. Results of Cases 1-6 with Panga. All columns in Table 3 correspond to those in Table 2.

	GLBD Solution Time (secs)	Total Enum. Time (secs)	GLBD Lower Bound	GLBD Increase Above Inherent	Optimal Risk	Gap between GLBD and Optimal	GLBD Gap
Case 1	502	41	4.266	0.8%	4.266	0%	0%
Case 2	522	306	4.575	8.1%	4.575	0%	0%
Case 3	> 7200	N/C	5.46	6.3%	N/C	N/C	355%
Case 4	> 7200	4070	5.401	0.7%	5.445	0.8%	286%
Case 5	> 7200	13092	5.824	8.6%	6.101	4.5%	427%
Case 6	> 7200	N/C	5.783	7.9%	N/C	N/C	573%

Table 4. Results of Cases 1-6 with Go-Fast. All columns in Table 4 correspond to those in Table 2.

As we can see from Cases 1 and 2 in Tables 4, 5, and 6, GLBD obtains the optimal solution in less than 10 minutes for small instances of DAM involving less than 300 missions. We also see that GLBD is slower than total enumeration of all possible solutions in DAM when such enumeration is feasible. We believe this occurs because the number of missions is small and the VBA-GAMS interface is rather inefficient. As for Cases 3, 4, 5, and 6, GLBD cannot obtain the optimal solution within two hours of run time for medium and large instances of DAM, involving several thousand missions. After two hours of calculations, we still observe a large gap between the upper and lower bounds in GLBD as displayed in Column seven in Tables 2, 3, and 4. However, as indicated by Cases 4 and 5, the solution obtained by GLBD in two hours tends to be close to the optimal risk (within 6%), regardless of attacker; see Column six in Tables 2, 3, and 4. Hence, even if the GLBD gaps are large due to weak upper cuts, GLBD can be used as a heuristic.

We collect the mission plans associated with the maximum risk output of GLBD, regardless if DAM produced the optimal solution or was stopped after two hours of calculations. Figure 9 shows a representative plot of mission plans for Cases 1, 2, 4, and 5. In Cases 1 and 2, i.e., cases where DAM produced the optimal solution, the mission plans have the defender platform patrol arcs associated with the two cells immediately to

the left of the attacker; the first cells for the attacker to move through, regardless of defender platform or attacker seacraft. Figure 9 illustrates Case 1's FFG mission plan against a Panga as a representative plan for Cases 1, 2, 4, and 5, since the optimal plans are similar, regardless of defender platform or attacker seacraft. The numbers 1, 2, and 3 correspond to the order of cell movement by the FFG. Therefore, in this example, the FFG first patrols the arc from cell (16,16) to cell (16,17) during the first time period of the FFG's mission, patrols the arc from cell (16,17) to cell (16,16) during the second time period of the FFG's mission, and patrols the arc from cell (16,16) to cell (16,17) during the third time period of the FFG's mission. In Cases 4 and 5, cases where DAM stopped after two hours of calculations, the mission plans were similar to Cases 1 and 2.

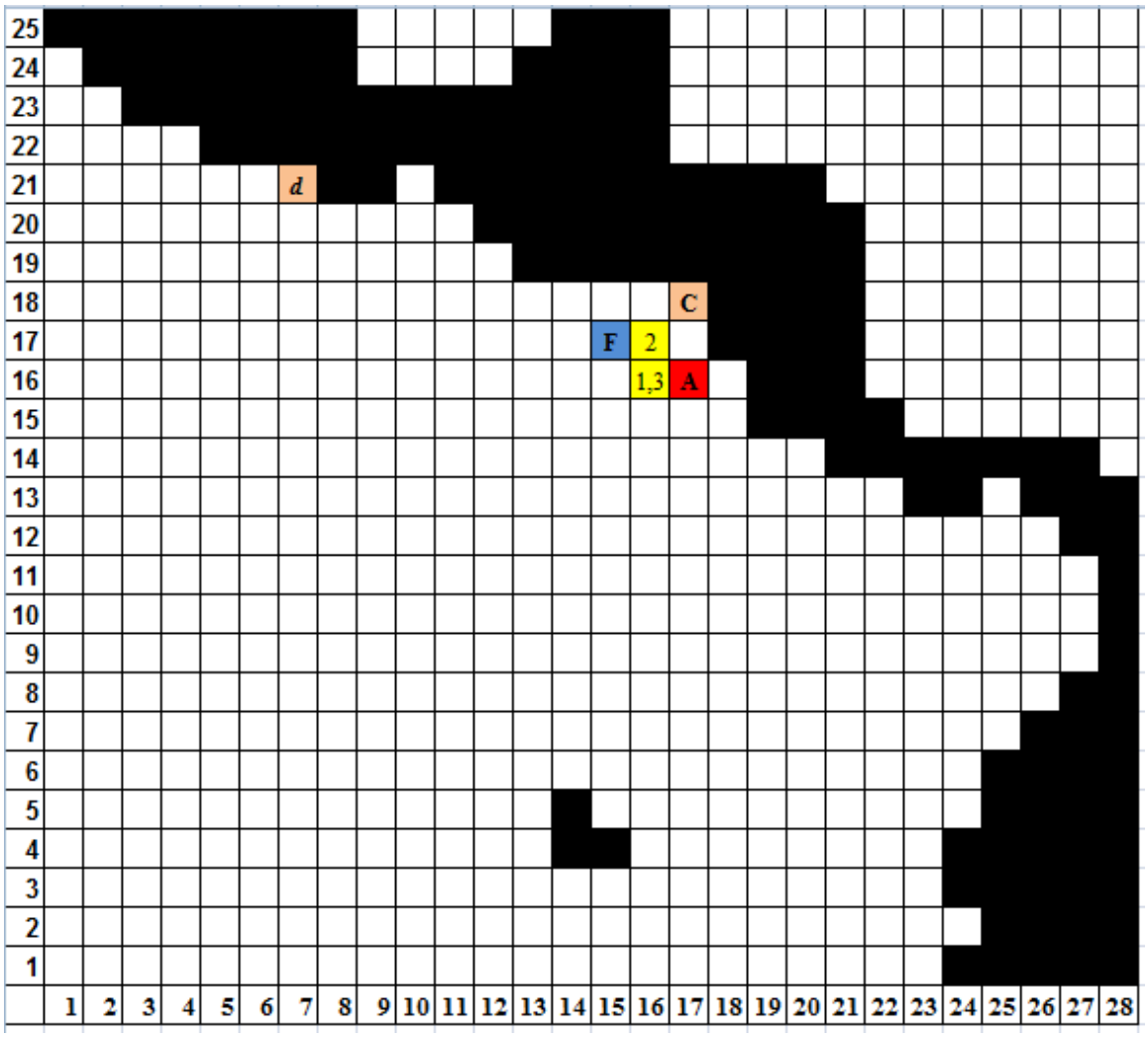

Figure 9. Snapshot of DAM mission plans, regardless of attacker. Cell "A" is the attacker, cell "C" is the Comalapa, Ecuador FOL (the only cell where the defender's P-3 and C-130 platforms originate), cell "*d*" is the attacker's default destination, and cell "F" is the defender's FFG. The numbers "1", "2", and "3" correspond to a representative sequence of cells in the defender's mission plan.

Figure 10 illustrates Case 3's mission plan, involving all three defender platforms, against a Panga as a as a representative plan for Cases 3 and 6, since the optimal plans are similar, regardless of defender platform or attacker seacraft. Cases 3 and 6 have mission plans with the defender platform patrolling the six cells immediately to the left of the attacker; the first six cell options for the attacker to move through. The numbers 1, 2, and

3 correspond to the order of cell movement described above. Interestingly, the defenders were layered so as to have the C-130 patrol the first two cells immediately to the left of the attacker, the P-3 patrol the two cells immediately to the left of the C-130, and the FFG patrol the subsequent two cells to the left of the P-3. This makes sense because the C-130 has the best probability of detection, the P-3 has the second best, and the FFG has the least.

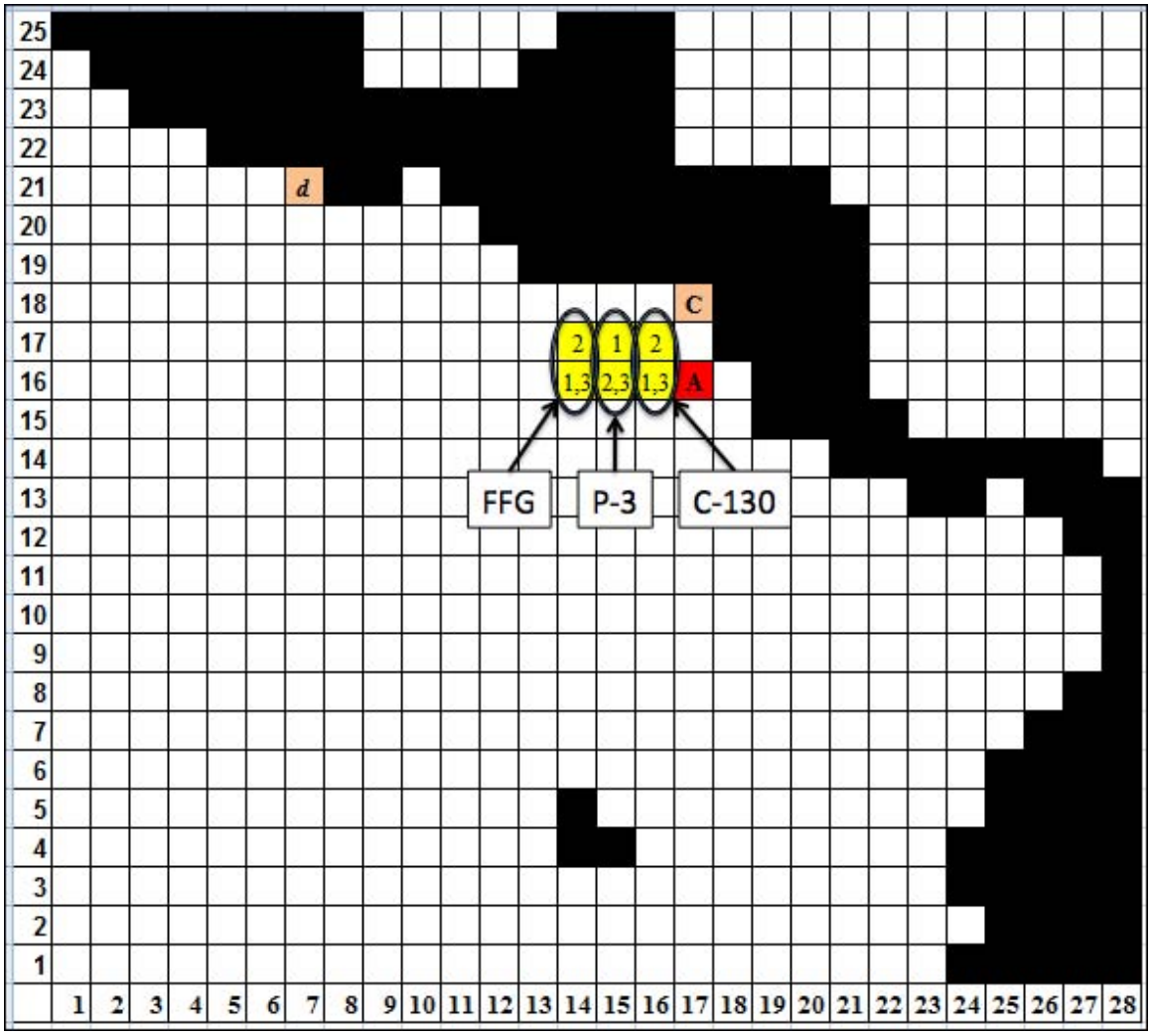

Figure 10. Snapshot of DAM mission plans, regardless of attacker. Cell "A" is the attacker, cell "C" is the Comalapa, Ecuador FOL (the only cell where the defender's P-3 and C-130 platforms originate), cell "*d*" is the attacker's default destination, and cell "F" is the defender's FFG. The numbers "1", "2", and "3" correspond to a representative sequence of cells in the defender's mission plan.

D. THE NEED FOR A TACTICAL DECISION TOOL

To gain a deeper insight into the difficulty in obtaining an optimal solution of DAM, we analyze data produced by total enumeration of Cases 4 and 5. To do this, we count the number of missions increasing the inherent risk by less than 10%, and divide this number by the total number of missions a defender platform can perform. Figure 11 illustrates these results. We note that the set of missions, M_l, includes missions of different duration. Hence, while the maximum allowable travel time, $t_{\max}$, for the attacker is 7 in Cases 4 and 5, the defender considers missions of shorter duration as the conservation of flight hours may be important for a decision maker. We see for Case 4 that regardless of platform, approximately 90% of one-time period missions result in less than a ten percent increase in inherent risk. The percentage of missions with substantial increase above the inherent risk increases as the number of time periods in a mission increases. This result is reasonable as the longer a defender performs a mission, the more arcs he can search and the more he can increase the risk. We see similar, but higher, percentages in Case 5. We believe these percentages are high because Case 4 has 3,998 possible missions and Case 5 has 12,730 possible missions. This result is in general agreement with JIATF-S, who estimates they do not detect the attacker in seven out of eight missions, an 87.5% failure rate (private communication with Sellers, 2010). Figure 11 indeed indicates that there typically exist a large number of missions which do not significantly increase the risk to the attacker above the inherent risk. This, of course, indicates the need for a model like DAM and an associated algorithm. It also makes it challenging to develop a Benders-type decomposition algorithm as cuts of this form, Equation (6), are typically weak.

Note that the difference between the Case 4 and Case 5 percentages in Figure 11, with many more missions in Case 5 resulting in an increase of inherent risk less than ten percent. At first glance, this seems counter intuitive since the air platforms have better radars than the frigate. Upon further investigation, we believe radars cannot be the source since both air platforms have different radars, yet the same percentages. We

believe the starting location of the defender relative to the attacker's location is the likely reason because both air platforms have the same starting location (the FOL) and the same speed.

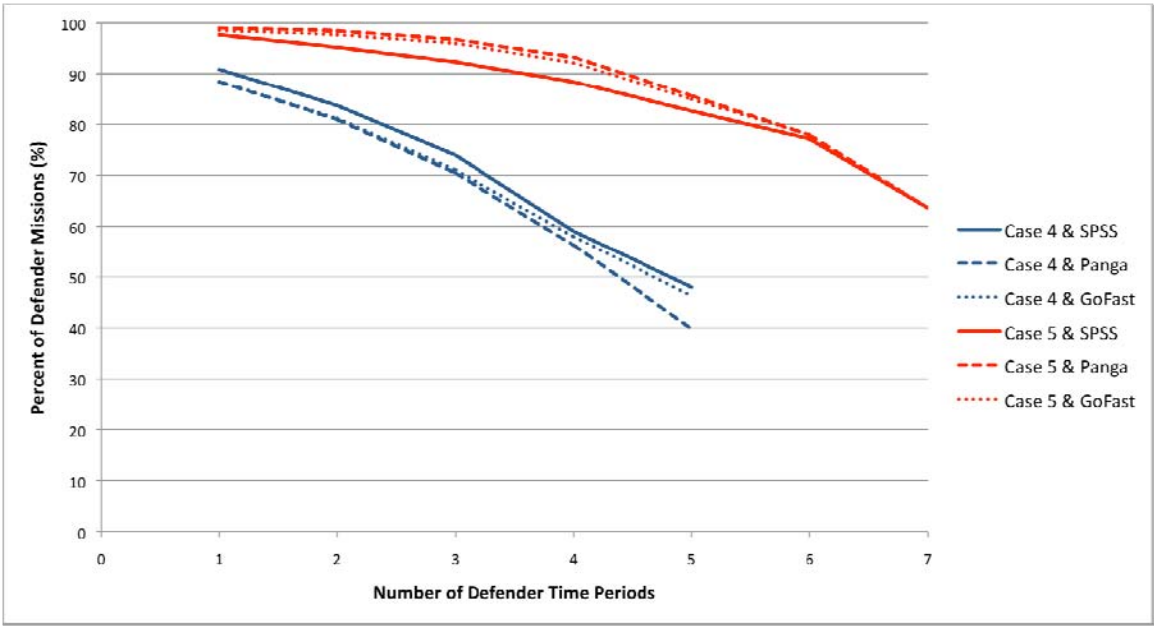

Figure 11. Percentage of defender missions increasing attacker risk less than 10% from inherent risk.

IV. CONCLUSIONS AND RECOMMENDATIONS

A. CONCLUSIONS

This thesis develops a model that prescribes the optimal defensive plan to maximize a smuggler's risk. We assume the smuggler intelligent and with imperfect knowledge of law enforcement platform locations but is aware that there is law enforcement that must be avoided. We demonstrate that through actionable intelligence, the Optimal Detection Problem can use a defender-attacker optimization model to maximize the smuggler's minimum risk through the optimal placement of three different types of law enforcement platforms against an intelligent smuggler, in one of three different types of seacraft. We demonstrate our defender-attacker model in the Eastern Pacific Ocean using three representative law enforcement platform types whose detection performance varies by platform and geography and three representative smuggler seacrafts whose risk varies by size and speed. In all of these cases, we find that further algorithmic development is needed to allow real-time use of this model and algorithm become a tactical level mission-planning aid to counter seacraft currently being used by drug smugglers.

We demonstrate in all cases, the DAM's solution is always greater than the inherent risk, and since 60%–98% of air missions and 40%–90% of frigate missions do little more than increase inherent risk by less than ten percent, we believe this would be a good initial recommendation for law enforcement allocation. We also demonstrate that the DAM is not fast enough to allow real-time use of this model and algorithm.

B. RECOMMENDATIONS

There are several interesting research avenues to be extended from this thesis. First, we recommend further algorithmic development needed to allow real-time use of this model and algorithm. Second, we show the largest increase in risk to the attacker comes from the early defender time periods (usually the second time period). Due to limitations on flight hours, and the high cost of flying hours, it would appear an optimal

employment policy for defender air platforms would be to limit air platform searches to only two time periods and return to the FOL, regardless of fuel or flight hours still remaining. We recommend further research into the feasibility and optimality of this type of policy in that may lead to better utilization of the defender platforms. Third, improved efficiency of our model can enable more time discretization and the analysis of larger scenarios. This would allow us to model the attacker's diagonal movements as well. Fourth, we recommend further analysis into researching a model to determine the number of time periods where the maximum risk will occur. Finally, we recommend further research into developing a model that can solve for multiple attackers simultaneously.

APPENDIX A. SENSOR PLATFORM PERFORMANCE ASSUMPTIONS AND DATA

This appendix presents the assumptions and data values used to determine the attacker's probability of survival $p_{ijt\omega_{ijt}}(x)$. This probability varies for each defender platform and each attacker platform. In general, we use the assumptions and rationale used by Pfeiff (2009). But, we use different assumptions and rationale for the Frigate search platform and shipping density.

A. MOVING SEARCH PLATFORM TYPES

The defender's platforms search arcs according to the missions they are assigned, as depicted in Figure 9. DAM only recommends the arcs (cells) to search, not the method of searching; that is decided by the defender operators. We assume that the probability of detection follows the random search formula:

$$p_{ijt\omega_{ijt}} = e^{-\sum_{l} w_{lij} v_l \lambda / A},$$

where w_{lij} is the sensor sweep width of defender platform l on arc (i, j), and v_l is the speed of defender platform l, both are presented in greater detail below. The time the attacker traverses an arc, λ, depends on the attacker's speed. We assume the SPSS speed is a constant 6 knots, the Panga speed is a constant 10 knots, and the Go-Fast speed is a constant 25 knots. Therefore, since all arcs measure 60nm, λ equals 10 hours for an SPSS, 6 hours for a Panga, and 2.4 hours for a Go-Fast. The defender searches half of cell *i* and half of cell *j* during time period *t*, therefore the area being searched, *A*, equates to 3600 nm^2. We assume defender platforms only detect attackers inside their assigned search cells.

1. P-3 *Orion* Maritime Patrol Aircraft

We assume the P-3 *Orion* to search at v = 180 nm/hr. We assume radar is the primary search sensor for the *Orion* and use this solely to determine the probability of

detection. The APS-137 radar is the primary search radar used by JIATF-S (private communication with Sellers, 2010). Table 1 is used to determine APS-137 sweep width, *w* (USCG, 2004).

Table H-27 Sweep Widths for Forward-Looking Airborne Radar (AN/APS-137)

16 Nautical Mile Radar Range Scale (Sweep Width in Nautical Miles)										
	On-scene Surface Winds (kts)									
Object Type	*< 5*	*to 10*	*to 15*	*to 20*	*to 25*	*to 35*	*to 45*	*to 55*	*to 65*	*> 65*
4 to 10 person life raft	12.1	8.6	3.1	0	0	0	0	0	0	0
17 to 25 foot recreational boat	13.6	11.9	8.2	2.8	0	0	0	0	0	0
26 to 35 foot recreational boat	16.6	16.3	15.4	14.2	12.6	9.5	3.9	0	0	0
36 to 50 foot recreational boat	21.0	20.7	19.9	18.9	17.5	14.7	9.8	3.5	0	0

32 Nautical Mile Radar Range Scale (Sweep Width in Nautical Miles)										
	On-scene Surface Winds (kts)									
Object Type	*< 5*	*to 10*	*to 15*	*to 20*	*to 25*	*to 35*	*to 45*	*to 55*	*to 65*	*> 65*
17 to 25 foot recreational boat	17.4	15.7	12.0	6.6	0	0	0	0	0	0
26 to 35 foot recreational boat	22.1	21.7	20.9	19.7	18.1	14.9	9.3	2.1	0	0
36 to 50 foot recreational boat	29.0	28.7	27.9	26.9	25.5	22.7	17.8	11.5	3.8	0

Table 5. APS-137 Sweep Widths (From USCG, 2004).

We assume *Orions* operating in 32nm radar range scale. We also assume the SPSS to have the same radar cross section as a 17-25 foot recreational boat, the Panga to have the same radar cross section as a 26-35 foot recreational boat, and a Go-Fast to have the same radar cross section as a 36-50 foot recreational boat. On-scene surface winds will vary from cell to cell, and time of year, based upon the surface wind data presented in Appendix B.

2. C-130 *Hercules* Maritime Patrol Aircraft

We assume the C-130 *Hercules* aircraft to search at v = 180 nm/hr. We assume radar is the primary search sensor for the *Hercules* and use this solely to determine the probability of detection. The APS-145 radar is the primary search radar used by JIATF-S (private communication with Sellers, 2010). We do not find a table of the APS-145 sweep width, so we derive the APS-145 sweep width, *w*, from the APS-137 sweep width. Radar range depends on a number of factors including target radar cross section. The APS-137 transmits power at approximately 500 kW (Pfeiff, 2009) and APS-145 transmits power at approximately 1 mW (Pfeiff, 2009). The APS-145 antenna area is roughly 20

times APS-137 antenna area (Pfeiff, 2009). Since the radar range varies by the fourth root of antenna area multiplied by transmission power, we apply a scalar of 2.5 to the APS-137 sweep width to obtain the estimated APS-145 sweep width (radartutorial.eu).

3. *Oliver Hazard Perry* Class Frigate (FFG) Surface Platform Type

We assume FFGs search at v = 10 nm/hr. We assume surface search radar is the primary search sensor for the FFG and use this only to determine the probability of detection. The AN/SPSS-55 is the primary surface search radar used by U.S. Navy FFGs. We did not find a table of the AN/SPSS-55 sweep width, so we derive the AN/SPSS-55 sweep width, w, from the APS-137 sweep width. Radar range depends on a number of factors including target radar cross section. The APS-137 transmits power at approximately 500 kW (Pfeiff, 2009) and AN/SPSS-55 transmits power at approximately kW (wikipedia, 2010). The AN/SPSS-55 antenna area is roughly the same size as the APS-137 antenna area (Wikipedia, 2010). Since the radar range varies by the fourth root of antenna area multiplied by transmission power, we apply a scalar of 0.7 to the APS-137 sweep width to obtain the estimated AN/SPSS-55 sweep width (Radartutorial.eu).

THIS PAGE INTENTIONALLY LEFT BLANK

APPENDIX B. GEOGRAPHIC MODEL ASSUMPTIONS AND DATA

This appendix presents the assumptions and data used to determine how the probability of detection varies by geographic location.

A. SURFACE WINDS

As discussed in Appendix A, surface winds influence radar sweep widths. We use a monthly average of surface winds taken from Special Sensor Microwave/Imager satellite data as a representative wind distribution for the Eastern Pacific Ocean (Remote Sensing Systems, 2010).

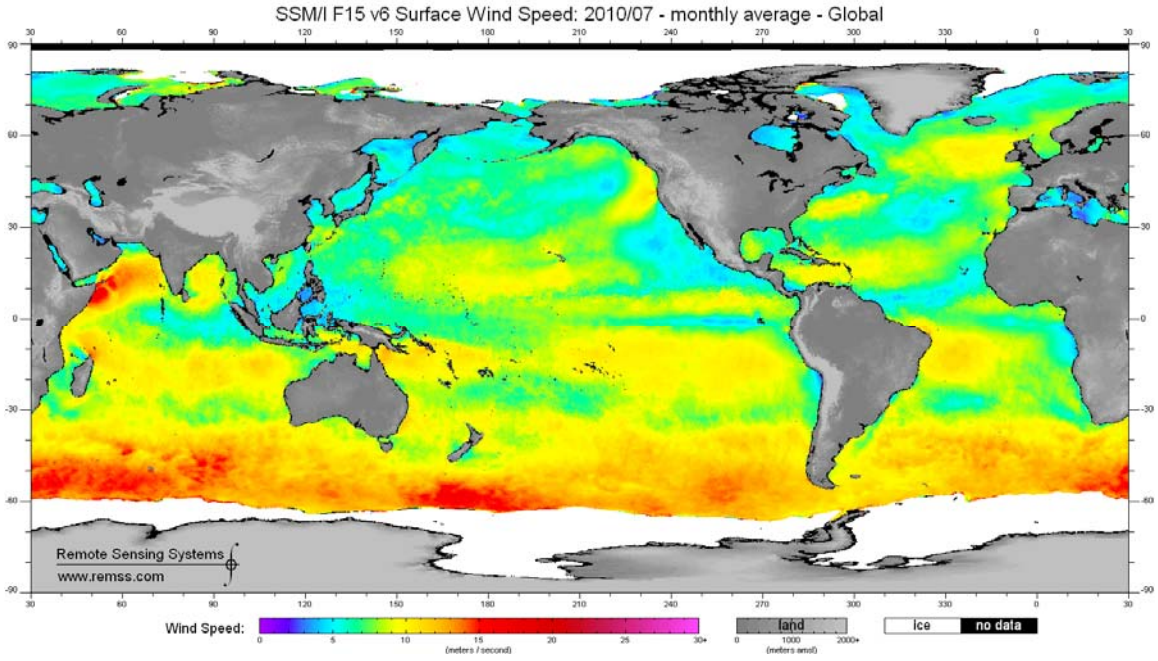

Figure 12. Monthly Average Surface Wind Speed July 2010 (From: http://www.remss.com/ssmi/ssmi_browse.html, 2010).

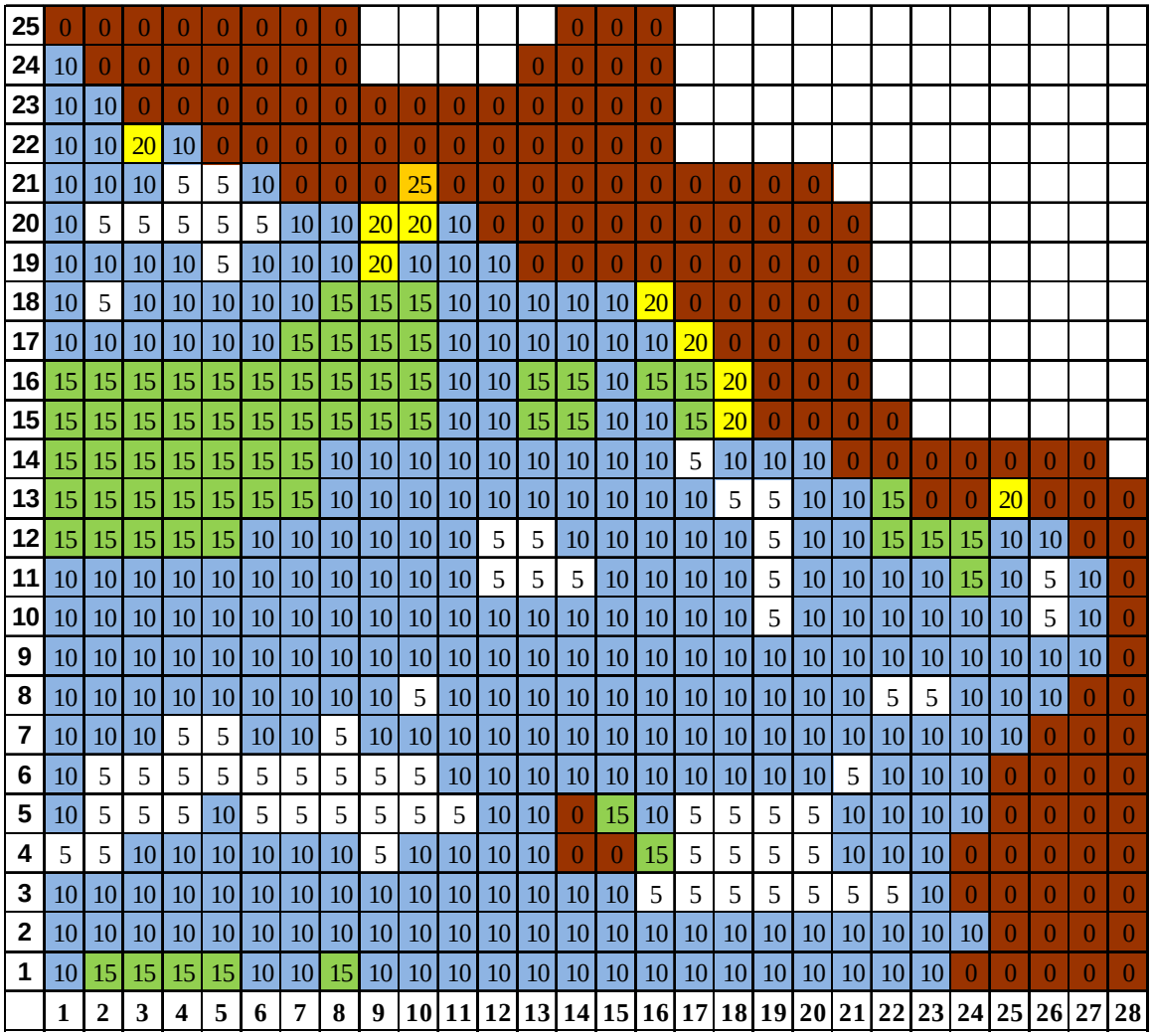

Figure 13. Monthly Average Surface Wind Speed July 2010 (From: http://www.remss.com/ssmi/ssmi_browse.html, 2010).

We use the monthly average winds from Figure 12 to construct the wind models shown in Figures 13.

B. COMMERCIAL SHIPPING TRAFFIC

It is unclear whether attackers prefer shipping lanes to blend in with neutral contacts or avoid shipping lanes due to potential contact reports (private communication with Sellers, 2010). Hence, we do not model commercial shipping traffic.

LIST OF REFERENCES

Benders, J. 1962. Partitioning procedures for solving mixed integer variables programming problems. Numerische Mathematik Vol. 4, 238–252.

Brown, G., M. Carlyle, J. Salmerón & K. Wood. 2006. Defending critical infrastructure. *Interfaces*, Vol. 36, No. 6, 530–544.

GAMS: A User's Guide, GAMS Development Corporation, Washington DC, 2010.

Dimitrov, N. & D. Morton. Combinatorial design of a stochastic markov decision process. In Dimitrov & Morton (Ed.) Book chapter in "*Operations research and cyber-infrastructure*." Springer 2009.

Dimitrov, N., M. Gonzalez, D. Michalopoulos, D. Morton, M. Nehme, E. Popova, E. Schneider & G. Thoreson. 2008. Interdiction Modeling for Smuggled Nuclear Material. Proceedings of the 49th Annual Meeting of the Institute of Nuclear Materials Management.

Joint Interagency Task Force-South (JIATF), 2010. Retrieved January 7, 2010 from http://www.jiatfs.southcom.mil/

The National Drug Intelligence Center (NDIC), 2010. National Drug Threat Assessment 2009. Retrieved January 7, 2010 from http://www.justice.gov/ndic/pubs31/31379/index.htm

Pfeiff, D. 2009. Optimizing Employment of Search Platforms to Counter Self-Propelled Semi-Submersibles. Master's Thesis, Naval Postgraduate School. Monterey, CA.

Radartutorial.eu, 2010. Retrieved August 9, 2010 from http://www.radartutorial.eu/01.basics/rb13.en.html

Remote Sensing Systems, 2010. Retrieved September 5, 2010 from http://www.remss.com/ssmi/ssmi_browse.html

Salmerón, J., K. Wood, & R. Baldick. 2009. Worst-Case Interdiction Analysis of Large-Scale Electric Power Grids. *IEEE transactions on power systems*, Vol. 24, No. 1, 96–104.

United States Coast Guard (USCG), 2004. SPSS Background. Retrieved January 7, 2010 from http://www.uscg.mil/Comdt/all_hands/docs/SPSS%20Background.pdf

United States Southern Command (USSOUTHCOM), 2010. Retrieved January 7, 2010 from http://www.southcom.mil/

Waller, S. and Ziliaskopoulos, A. 2002. On the Online Shortest Path Problem with Limited Arc Cost Dependencies, Vol. 40, Issue 4, 216–227.

Washburn, A. and K. Wood. 1995. Two-Person Zero-Sum Games for Network Interdiction. *Operations research*, Vol. 43, Issue 2, 243–251.

Wikipedia, 2010. Retrieved September 5, 2010 from http://www.wikipedia.org

Wood, K. 1993. Deterministic Network Interdiction. Mathematical and Computer Modeling, Vol. 17, No. 2, 1–18.

INITIAL DISTRIBUTION LIST

1. Defense Technical Information Center
   Ft. Belvoir, Virginia

2. Dudley Knox Library
   Naval Postgraduate School
   Monterey, California

3. Dr. Donald Wagner
   Office of Naval Research
   Arlington, Virginia

4. Professor Johannes O. Royset
   Naval Postgraduate School
   Monterey, California

5. Professor Javier Salmerón
   Naval Postgraduate School
   Monterey, California

6. CAPT Jeffrey Kline, USN (Ret.)
   Naval Postgraduate School
   Monterey, California